CHAPTER 2

A MODEL FOR SURF BEAT

P.J. van Leeuwen[1] and J.A. Battjes[1]

Abstract

A model is presented for the generation of low-frequency waves propagating normal to the beach. The input parameters are the bottom profile and the variance spectrum of the incoming wind waves. The model predicts the variance spectrum of the low-frequency waves. Also correlations between e.g. wind wave envelope and low-frequency surface elevation can be calculated. Results of the model are compared to field data.

1 Introduction

When wind waves approach mildly sloping beaches, a significant amount of energy can be found at frequencies an order of magnitude lower than those of the incoming wind waves. Part of this low-frequency energy can be ascribed to edge waves, whose phase variation is alongshore. An important part however can be assigned to two-dimensional shorenormal waves, which are here called surf beat.

The first observations of surf beat were made 40 years ago by Munk (1949). He found a linear relation between the amplitudes of the low-frequency waves and those of the wind waves. Looking at the time records of both types of waves he found that the low-frequency waves lagged behind the wind wave envelope with about 140 seconds, which he attributed to the time needed for the wind wave envelope to travel to the surf zone and for the low-frequency waves to travel back to the wave recorder. Tucker (1950) reported the same kind of measurements, but he used correlograms to analyze his data. He also found that the low-frequency waves are lagging behind the wind wave envelope, and that the largest absolute value of the correlation coefficient occurs when this coefficient is negative. This means that the wind wave envelope and the low-frequency waves are 180 degrees out of phase, apart from travel considerations.

Biésel (1952) proved theoretically that groups of short waves are accompanied by nonlinear long waves, bound to these groups. Longuet-Higgins and Stewart (1964) clarified this theoretical result with the concept of radiation stress. Due to this nonlinear effect, water is pushed away from areas with high waves and accumulated

1 Delft tech. Univ., Dept. of Civil Engineering, Delft, The Netherlands.

under low waves. This results in long waves, bound to the wind wave groups. An important feature is that the bound long waves are 180 degrees out of phase with the wind wave envelope. A way to explain the observations by Munk (1949) and Tucker (1950) qualitatively is to suppose that the bound long waves are reflected in the surf zone, and propagate seaward as free long waves. Since the paper pays no attention to the mechanism of reflection, it is difficult to compare the theoretical results with experiments.

Quantitative models were lacking until 1981. The relatively simple case of bichromatic wind waves is here addressed first. Lo (1981) presented a bichromatic model which calculates in the time domain and in which he could explain the linear relation between the low-frequency wave amplitude and the wind wave envelope height by taking the generation of low-frequency waves due to the breaking of the regular wave groups into account. He found that the surf zone region was very important for low-frequency wave generation, and that the smaller the beach slope, the higher the surf beat wave heights. The reason for this is that more time is available for the energy transfer from the wave groups to the low-frequency waves. Lo (1981) did not mention how the forcing of the low-frequency waves due to wave breaking was modelled.

Symonds et al. (1982) investigated the forcing of low-frequency waves by the time variation of the location of the break point. This variation gives rise to a time-varying set up and hence produces low-frequency waves. The analysis was performed for bichromatic short waves with periodic wave groups. The difference between this model and that of Lo (1981) is that the calculations are done in the frequency domain and that the bound long waves are ignored. Kostense (1984) verified this model in a wave flume and found good qualitative agreement.

Schäffer and Svendsen (1988) presented a spectral bichromatic model in which they allow for wave height modulations after the waves are broken by taking a fixed (in space) break point. The model uses both the bound long waves and the long wave generation due to wave breaking, but because of the wave modulations inside the breakpoint bound long waves are generated in this region too. In a later paper by Schäffer and Jonsson (1990) the model is compared with the Kostense (1984) data. An overestimation of the outgoing low-frequency wave amplitude was attributed to bottom friction, which is not included in the model. This is the only model which allows for wave height modulations inside the surfzone and the consequent generation of low-frequency waves in this region.

The calculation of surf beat using random wind waves was first addressed by Lo (1981). He uses both types of forcing of low-frequency waves and calculates in the time domain. A comparison of his model with field data by Goda (1975), using a full wind wave spectrum as input, showed the right order of magnitudes for the low-frequency spectral components.

List (1990) also proposed a model for random wind waves in which both generating mechanisms are present and in which the calculations are done in the time domain. The model uses as input measured wind wave envelope time series, from which low-frequency wave time series are calculated. A comparison with field data showed results for the low-frequency wave energy levels which are 5 to 50% off, and good qualitative results for the correlation between wind wave envelope and low-frequency surface elevation.

The present paper also deals with low-frequency wave generation by random wind waves. The main difference with the models of Lo (1981) and List (1990) is that the calculations are here performed in the frequency domain. The input of the model is the energy spectrum of the wind waves, the idea being that the low-frequency energy spectrum is not dependent on one specific realisation of the process described by the energy spectrum of the wind waves.

In the present paper the theoretical model is developed first. Then a few remarks are made about the collection and the processing of the field data, used for comparison with model results. The next section deals with the comparison and a discussion of the results. Some concluding remarks close the paper.

2 The model

The basic philosophy behind the model is to combine the ideas of Longuet-Higgins and Stewart (1962) and Symonds e.a. (1982), and to extend them to the case of wind waves with a continuous spectrum. A spectral approach will be followed, because usually input information is in that form, and not in the form of time series. The basic equations are the linearized shallow water equations. After elimination of the velocity a second order partial differential equation results for the low-frequency surface elevation (see e.g. Symonds e.a. 1982):

$$\frac{1}{g}\zeta_{tt} - h_x\zeta_x - h\zeta_{xx} = -\frac{1}{g\rho}S_{xx} \qquad (1)$$

in which ζ is the low-frequency surface elevation, h the mean water depth, ρ the water mass density, g the acceleration of gravity and S the radiation stress. The subscripts denote partial differentiation. The driving term for the low-frequency waves is the second space derivative of the radiation stress. Because the wind waves have a continuous spectrum the radiation stress is randomly varying.

The idea is now to expand the variables in a Fourier-Stieltjes (FS) integral according to

$$a = \int_0^\infty e^{i\omega t}\, dA$$

in which dA is a random increment function for an interval $d\omega$. It can be seen as the complex amplitude of the waves in a frequency interval $d\omega$ and is related to the variance spectrum G_{aa} of a by

$$G_{aa}\, d\omega = \frac{1}{2} < dA\, dA^* > \qquad (2)$$

where < .. > indicates ensemble averaging, and the asterisk denotes the complex conjugate.

For the FS transformed long wave equation one now finds

$$\frac{\omega^2}{g} dZ(x,\omega) + h_x dZ_x(x,\omega) + h dZ_{xx}(x,\omega) = -d\phi_{xx}(x,\omega) \tag{3}$$

in which dZ is the FS transform of the low-frequency surface elevation ζ, and $d\phi$ the FS transform of the forcing. First note that equation (3) is a second order ordinary differential equation, which is much easier to solve than its partial counterpart. For instance in the case of a plane sloping bottom, the solution of (3) is found as a combination of integrals over Bessel functions of first and second kind.

The calculation of the forcing term in equation (3) needs extra attention. Because it is a complex quantity its absolute value as well as its phase has to be calculated.

The phase will be space and frequency dependent. The frequency dependence of the phase cannot be determined because only the wind wave variance spectrum is given. However, we want to calculate the variance spectrum of the low-frequency waves so this frequency dependence is of no importance. The space dependence of the phase of the forcing will be important. The forcing will have a phase shift along the spatial coordinate due to the fact that the forcing is related to the wind wave envelope squared via the radiation stress. Because it takes the wind wave envelope some time to pass through the surf zone, a certain distance Δx corresponds to a phase shift $\Delta\psi$ in the forcing. A way to calculate this phase shift is to assume that the wind wave envelope travels with group velocity C_g of the peak frequency. The phase shift due to the finite travel time of the wind wave envelope now becomes

$$\Delta\psi(x - x_0) = \arg\{d\phi(x,\omega)\} = \int_{x_0}^{x} \frac{\omega}{C_g} dx \tag{4}$$

The absolute value of the forcing term in equation (3) will be calculated from the variance spectrum of the forcing which in turn will be determined from the variance spectrum of the wind waves. As mentioned above, the forcing term is proportional to the second space derivative of the radiation stress, which in turn is proportional to the wave envelope R squared. Consequently, the variance spectrum of the envelope squared has to be determined to obtain the variance spectrum of the forcing. A way to calculate the variance spectrum of the wind wave envelope squared is to start from the covariance of two squared envelopes:

$$C[R^2(t), R^2(t+\tau)] = E[R^2(t) R^2(t+\tau)] - E^2[R^2(t)] \tag{5}$$

in which C .. is the covariance, and E .. is the expected value operator. The Fourier transformation of the covariance gives the required variance spectrum.

The expected values in equation (5) can be found from the joint probability density $p(R_1, R_2)$ of two envelopes at a time lag τ. For a narrow-band Gaussian process, this probability density has been derived by Rice (1944, 1945). It has since been called the 2-D Rayleigh distribution. This density has been used successfully by Kimura (1980) in his description of wave groups. In the case of breaking waves the probability density $p(R_1, R_2)$ has to be modified because the wave height is limited to a critical value, mainly determined by the local depth. A truncated 1-D Rayleigh distribution developed and used successfully by Battjes and Jansen (1978) to determine the mean energy dissipation in breaking waves is adopted here, extended in a straightforward manner to the two-dimensional case.

Now that the variance spectrum of the forcing has been found in which both breaking and nonbreaking waves are incorporated, the variance spectrum of the low-frequency waves can be obtained by solving the ordinary differential equation (3) and using (2).

The method outlined above also gives one the opportunity to calculate correlation coefficients, for instance for the correlation between low-frequency surface elevation and wind wave envelope. At first sight this may seem impossible because the frequency dependence of the phases of the spectral components of e.g. low-frequency surface elevation is not known. To solve this problem it is noted that only the phase difference between the FS transform of the low-frequency surface elevation and the FS transform of the wind wave envelope at each frequency has to be known, not the phase difference between different spectral components. The required phase differences at each frequency follow directly from differential equation (3).

3 Data collection and processing

The data used are from a field experiment conducted at the U.S. Army Corps of Engineers Field Research facility in Duck, North Carolina, U.S.A., on September 9, 1500 EST 1985. The beach was approximately two-dimensional. A cross-shore array of eight pressure sensors and bi-axial horizontal current meters provided time series with a sample rate of 2 Hz. Figure 1 shows the bottom profile with the positions of the sensors. The pressure sensors were of the diaphragm type and the current meters were Marsh McBirney electromagnetic meters.

The data describe swell with highly grouped waves and a narrow spectral peak near 0.08 Hz. The root mean square wave height was 0.4 m. This data set was chosen because of the profound group structures present during the measurements and the nearly shorenormal incidence.

The low-frequency wave band is defined as $0.007\text{Hz} < f < 0.03\text{Hz}$, because outside this region the waves were found to be uncorrelated with the wave groups. Low-frequency standard deviations were calculated from the pressure sensors at each of the sensor locations. The cross-correlation coefficient between wind wave envelope and incoming and outgoing low-frequency waves at a sensor location outside the surfzone ($x = 222\,\text{m}$) was calculated. The wind wave envelope was found by calculating the Hilbert transform of the time series, using an approximate temporal Hilbert filter given by McClellan et al. (1979), with 95 points (Pierce, 1985). The low-frequency waves were obtained by lowpass filtering the time series and separated into incoming and outgoing waves using the method proposed by Guza et al. (1985):

$$\zeta_{in} = \frac{\zeta + \sqrt{\frac{h}{g}}U}{2} \quad , \qquad \zeta_{out} = \frac{\zeta - \sqrt{\frac{h}{g}}U}{2} \tag{6}$$

in which ζ is the low-frequency surface elevation and U is the low-frequency orbital velocity defined positive offshore.

As mentioned before, the model needs as input the variance spectrum of the wind waves. This was obtained by a Fourier transform of the time series from the seawardmost sensor.

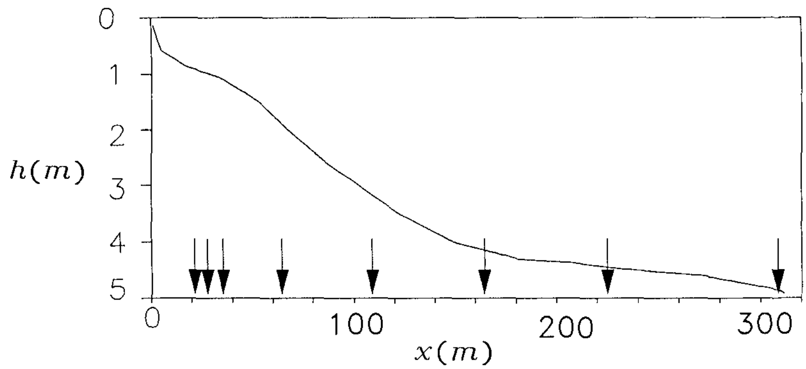

Figure 1 Bottom profile, arrows indicate sensor locations.

4 Comparison and discussion

To verify the model, both field data and laboratory data will be used. In this paper only field data are used to test the model. The first test uses the standard deviation of the outgoing low-frequency waves $\sigma_{\zeta_{out}}$. The second uses the correlation between wind wave envelope and surface elevation of the incoming and outgoing low-frequency waves.

The ratio of breaker height to local depth, γ, is a free parameter in the model. It has been set equal to 0.4. However, a change in γ does not give a strong change in the results presented here.

The reason for the test using the standard deviation of the outgoing low-frequency waves is the following. The outgoing low-frequency waves are a combination of low-frequency waves of three different origins: waves, which were first incoming and bound to the wave groups, and then reflected on the beach to become outgoing; waves which are produced by the time-varying breakpoint mechanism as outgoing waves, and finally waves which are produced by the time-varying breakpoint mechanism as incoming waves, and which then are reflected by the beach to become outgoing. If a model can reproduce the energy level of this complicated mixture within the error margins (5% in this case) without tuning parameters (except maybe γ), the physics in that model can be close to the real physics involved. Of course, more situations have to be used as test cases for the 'can' to be a 'must'.

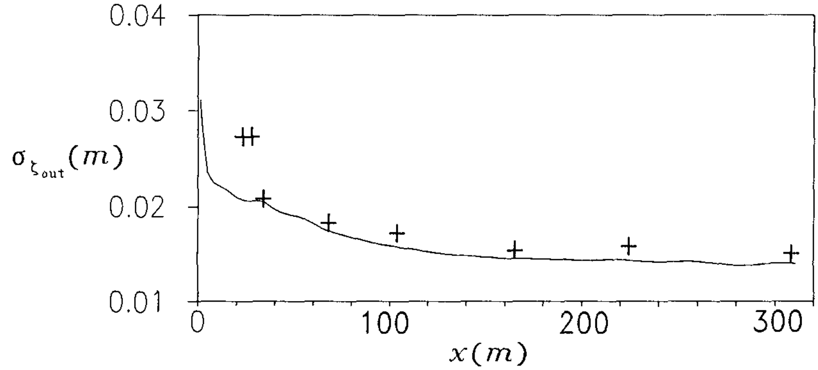

Figure 2 Standard deviation of surface elevation of outgoing low-frequency waves as function of distance from the water line. (+) data, (-) theory.

In figure 2 the standard deviation of the outgoing low-frequency surface elevation is given as function of the distance from the shore line. The surfzone extends to about 60 m from the water line. The model shows good agreement with the data from six sensors. Unfortunately the two innermost pressure sensors have spurious energy in the low-frequency band, so that the comparison in this region is not conclusive. The reason that some energy must be spurious is that these sensors both show a large peak at a different frequency, with a spectral energy density as high as that of the wind waves, while outside the surfzone these peaks are not observed. In principle it could be possible that some unknown forcing mechanism for low-frequency waves is active inside the surfzone, the waves of which are cancelling each other somehow when they try to leave the surfzone. It is noted however that the beach does not have a certain length scale, like a bar, so this might be unlikely to happen on this beach.

Figure 3a shows the correlation coefficient for the wind wave envelope and the surface elevation of the incoming low-frequency waves. The 95% confidence interval on zero correlation was found to be below 0.09 for the data. A strong negative peak can be observed at zero lag, which must be attributed to the bound low-frequency waves. The fact that the peak from the field data is not that pronounced shows that the bound low-frequency waves are not the only low-frequency waves with a shorenormal particle velocity component. Probably edge waves and shore-oblique leaky mode waves are present.

Figure 3b shows the correlation coefficient for the wind wave envelope and the surface elevation of the outgoing low-frequency waves. Again the 95% confidence interval on zero correlation was found to be below 0.09 for the data. A strong negative peak can be seen in the theoretical curve at a time lag of about 100 s, which is precisely the time needed for the bound long waves to travel to the beach (at the still-water line), reflect from the beach, and travel back as free waves to the pressure sensor again. The data also show a peak at this time lag. The theory additionally shows significant oscillations at smaller and larger time lags. The reason for this is not entirely clear yet. The negative peak at about 62 s time lag may be associated with the outgoing waves produced by the time-varying breakpoint mechanism. This time lag corresponds to the time needed for the wave envelope to travel to the 'mean' breakpoint and for the generated low-frequency waves to travel back to the sensor. The 'mean' breakpoint is here defined as the point in which the rms wave height is maximum. The data do not show significant correlations at this time lag.

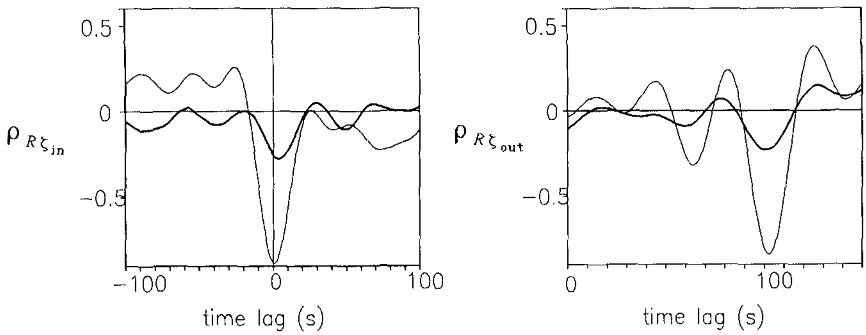

Figure 3 Cross correlations between wind wave envelope and low-frequency surface elevation at x=222 m. a) incoming low-frequency waves, b) outgoing low-frequency waves. The thick line represents the data, the thin line represents the theoretical results.

5 Conclusions

A model has been developed for the generation of shorenormal low-frequency waves by random wind waves. The model needs as input the energy spectrum of the wind waves, and calculates in the frequency domain. The results of the model are compared to field data.

The comparison showed that the measured low-frequency standard deviations at a range of distances from the water line are predicted within their error margins. However the innermost pressure sensors are believed to contain spurious low-frequency energy, so the comparison was not conclusive in this region.

The time lag of strongest cross-correlation between wind wave envelope and incoming and outgoing low-frequency waves is predicted correctly, although the magnitude of the correlation coefficient is overestimated. The remaining structure of the theoretical cross-correlation function requires further investigation.

Acknowledgements

The investigations were supported by the Working Group on Meteorology and Physical Oceanography (MFO) with financial aid from the Netherlands Organization for the Advancement of Research (N.W.O.). The U.S. Army Corps of Engineers is thanked for the DUCK85 field data from their Field Research Facility in Duck, North Carolina, U.S.A..

References

Battjes J.A. and J.P.F.M.Jansen (1978), Energy loss and set up due to breaking of random waves. *Proc. 16th Coastal Eng. Conf. ASCE,* 569-587, Hamburg.

Biésel F. (1952), Equations générales au second ordre de la houle irrégulière. *La Houille Blanche,* 7, 372-376

Kimura A. (1980), Statistical properties of random wave groups. *Proc. 17th Coastal Eng. Conf. ASCE,* 2955-2973, Sydney.

Kostense J.K. (1984) Measurements of surf beat and set down beneath wave groups. *Proc. 19th Coastal Eng. Conf. ASCE,* 724-740, Houston.

List J.H. (1990) A model for two-dimensional surf beat. *Submitted for publication.*

Lo J-M. (1981) Surf beat: numerical and theoretical analysis. *Ph.D. Dissertation,* University of Delaware.

Longuet-Higgins M.S.and R.W. Stewart (1964), Radiation stresses in water waves; a physical discussion, with applications. *Deep Sea Res.,* **11**, 529-562.

Munk W.H. (1949), Surf beat, *EOS Trans. AGU.,* **30**, 849-854.

Rice S.O. (1944, 1945) Mathematical analysis of random noise. *Bell System Technical Journal,* **23, 24.**

Schäffer H.A. and I.A.Svendsen (1988) Surf beat generation on a mild-slope beach. *Proc. 21st Coastal Eng. Conf. ASCE,* 1058-1072, Malaga.

Schäffer H.A. and I.G. Jonsson (1990) Theory versus experiments in two-dimensional surf beat. *Presented at the 22nd International Coastal Eng. Conf. ASCE,* Delft.

Symonds G., B.A. Huntley and A.J. Bowen (1982), Two-dimensional surf beat: Long wave generation by a time-varying breakpoint, *J. Geophys. Res.,* **87**, 492-498.

Tucker M.J. (1950), Surf beats: Sea waves of 1 to 5 minutes' period, *Proc. Roy. Soc., Ser A,* **202**, 565-573.